Supplementary Information

Regulating the electrolyte network to accelerate reversible I^-/I_2Br^- conversion and suppress zinc dendrite formation in advanced zinc-iodine flow battery

Ruhan Zhao[a,1] Ke Lu[b,1], Mohsin Pasha[c], Rongqian Kuang[a], Hong Zhang[a,1,*], Songtao Lu[a,1,*]

[a]MIIT Key Laboratory of Critical Materials Technology for New Energy Conversion and Storage, School of Chemical Engineering and Chemistry, Harbin Institute of Technology, Harbin, Heilongjiang 150001, China.
*E-mail: zhanghonghit@hit.edu.cn (H.Z.); lusongtao@hit.edu.cn (S.L.)
[b]Institutes of Physical Science and Information Technology, Anhui University, Hefei, Anhui 230601, China.

[c]School of Chemistry and Chemical Engineering, Shanghai Jiao Tong University, Shanghai 200240, China.

[1]R.Z. and K.L. contributed equally to this work.

Sample preparation

Preparation of ZBAWn： The ZBAWn eutectic electrolyte was synthesised using a simple heated mixing method, where 0.02 mol $ZnBr_2$ and 0.06 mol Acetamide were mixed and then stirred at 60 °C for 60 min to obtain a homogeneous mixture. Moreover, by adding 0.02/0.06/0.12/0.16/0.306/0.32 mol of water and stirring for 30 min at room temperature, the ZBAs were designated as ZBAWn (n=1, 3, 6, 8, 15.3, 16).

Preparation of ZBA-I： Firstly, 0.02 mol $ZnBr_2$ and 0.06 mol Acetamide were mixed and heated to 60 °C and stirred for 60 min. Then 0.04 mol of I_2 was added to the mixture and stirring was continued for 3 h. Afterwards, water was added until the concentration of Zn^{2+} in the solution reached 2 mol L^{-1} and stirred for 3h at room temperature, and the solution was designated ZBA-I.

Sample characterization

Materials characterizations: The morphology of the carbon felt and zinc anode was characterized by scanning electron microscopy (SEM, ZEISS). The crystal structure of the zinc anodes was characterized by X-ray diffraction (XRD) on a Bruker D8-Advance X-ray diffractometer (Cu Kα, λ=1.5406 Å), and diffraction data was collected for 2θ angles from 10° to 80°. Electrospray ionization mass spectra (ESI-MS) were collected by using Thermo Scientific Q Exactive in negative ion mode. Fourier transform infrared spectroscopy (FTIR) spectra were acquired using a Nexus system and UV-vis spectroscopy spectra were obtained using a METASH Model 8000 spectrometer. Raman spectra were obtained using a RENISHAW spectrometer with a laser source at a wavelength of 532 nm. The contact angle was tested using a contact angle tester (OCA25, DATAPHYSICS). UV-vis spectroscopy spectra were obtained using a METASH Model 8000 spectrometer. The viscosity and ion conductivity of eutectic electrolyte were determined by NDJ-8S (CNSP, Shanghai) and DDSJ-319L (Leici, Shanghai).

Electrochemical measurements

An electrochemical workstation (CHI660E, CH Instruments) and a conventional three-electrode cell equipped with a glassy carbon electrode (active area of 0.07 cm^2), a platinum foil counter electrode and a SCE (0.241 V vs. the standard hydrogen electrode, SHE) reference electrode were used for CV, LSV, EIS, and CA tests. LSV was displayed at a scan rate of 5 mV s^{-1} to minimise the effect of capacitance. CA was performed at an applied potential of +0.8 V, and EIS was performed at an applied potential of +0.45, with the aim of fully competing I^-/I_2 and I^-/I_2Br^- couples. The Zn||Zn cells using CR2025-type cells were assembled by the Zn metal anode (Φ10 mm), 100 μL electrolyte, glass fiber separator (Whatman, GF/D) on Neware battery test system to obtain cyclic performance at 1mA cm^{-2}, 1mAh cm^{-2}, after which Tafel plots were obtained by using CHI660E.

Flow cell measurements

For ZIFB-Br, 2M $ZnBr_2$ + 4M I_2 and 2M $ZnBr_2$ were used as positive and negative electrolytes with 10 ml for catholyte and 20 ml for anolyte, respectively. For ZBAFB, ZBA-I and ZBAW15.3 were used as positive and negative electrolytes with 7 ml for catholyte and 14 ml for anolyte, respectively. The positive and negative electrodes were made of 3*4.5 cm commercial carbon felt. Zn foil was added on the anode side to provide excess Zn. The separator was made of Ketjent black modified Nafion 117 membrane and was immersed in ZnBr2 solution at 60°C for 3 hours before use.The peristaltic pump is provided by Shenchen Ltd. and the battery system and carbon felts are obtained by Zhisheng Ltd. Cyclic stability tests, rate performance and polarisation curves of the cells were carried out using Neware battery test system.

Computational Simulation Details

The molecular dynamics (MD) simulations were conducted using the Forcite analysis tool within Materials Studio to investigate the solvation structure of Zn^{2+}. Electrolyte molecules were arranged in a periodic box to form bulk systems, with the compositions of the simulated electrolytes detailed in the table below. Initially, all electrolyte systems were relaxed using the microcanonical ensemble (NVE) at 300.0 K for 500 ps. Subsequently, the equilibrium density and volume were simulated using constant-pressure, constant-enthalpy ensemble (NPH) and canonical ensemble (NVT) MD for 1.0 ns at 300.0 K and 1 bar pressure to minimize the energy of the initial structure. The final system structure was obtained through constant-pressure–constant-temperature (NPT) MD simulations for 5.0 ns with a 1.0 fs time step. The radial distribution functions (RDFs) and statistical summary of hydrogen bonds were derived from the final structures using the Forcite analysis tool. Binding energy simulations were carried out using the B3LYP method in the DMol3 module of Materials Studio, as per the following equation:

$$E = E_{total} - E_{Zn^{2+}} - E_n$$

where E_{total} is the structure total energy, $E_{Zn^{2+}}$ is the energy of zinc ion, and E_n is the energy of different molecule fragments (X = Br^-, Ace, H_2O). The convergence tolerances of the systems were set to 1.0×10^{-5} eV/atom for energy, 0.002 Ha/Å for maximum force, and 4.5×10^{-3} Å for maximum displacement.

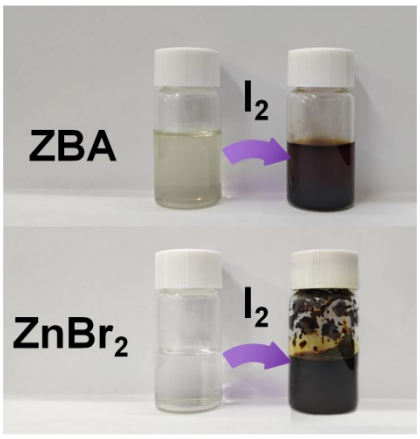

Figure S1. Photographs of the color change of ZBA before and after I_2 adding.

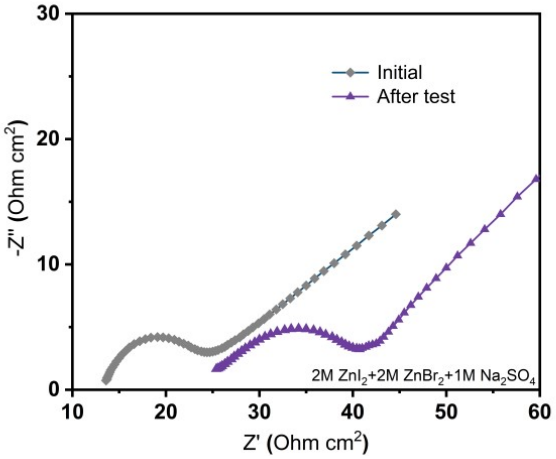

Figure S2. EIS plot of the aqueous electrolyte before and after CA test

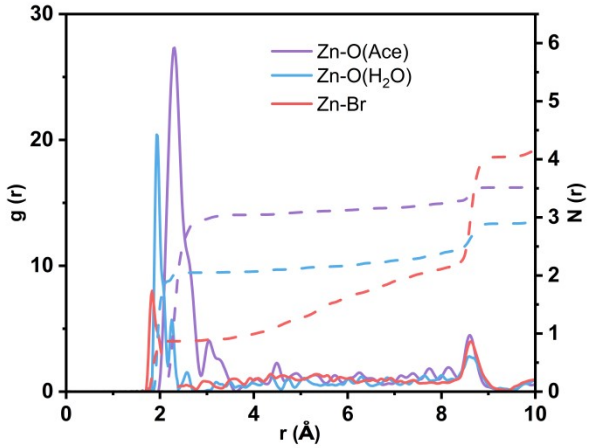

Figure S3. RDFs for Zn-Ow (H_2O), Zn-O (acetamide), Zn-Br, and corresponding coordination number of Zn^{2+} collected from MD simulations in ZBA-I.

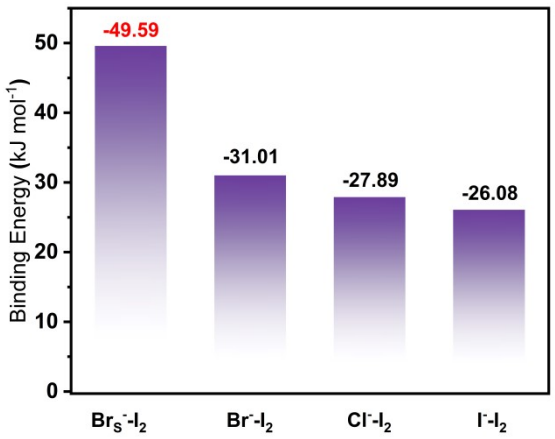

Figure S4. Binding energy of solvated Br^--I_2 in ZBA-I, Br^--I_2, Cl^--I_2, and I^--I_2.

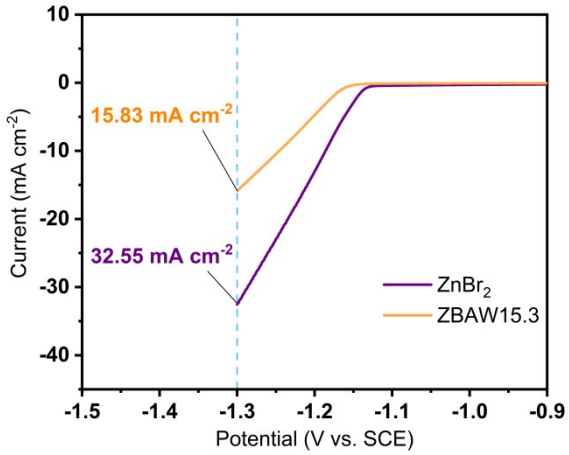

Figure S5. LSV curves of 2.0 M $ZnBr_2$ and ZBAW15.3.

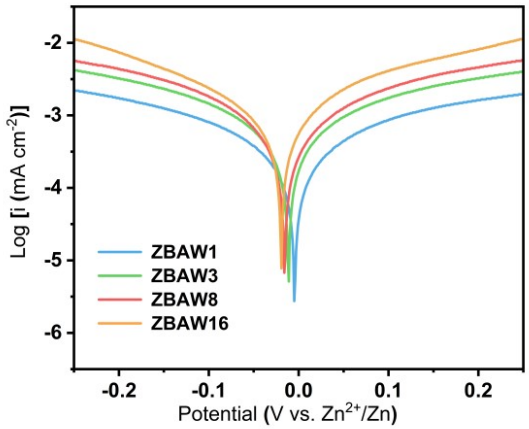

Figure S6. Tafel plot of ZBA electrolyte with various water content.

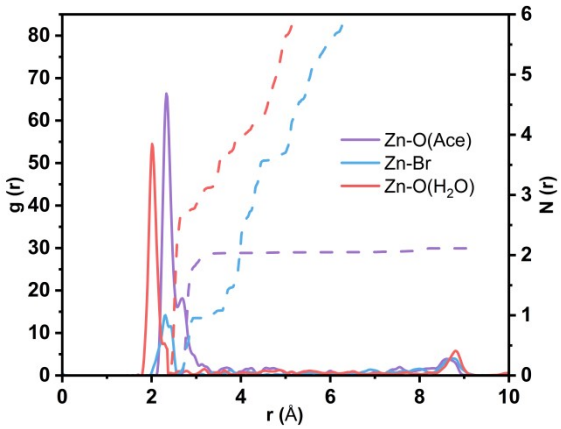

Figure S7. RDFs for Zn-Ow (H_2O), Zn-O (acetamide), Zn-Br, and corresponding coordination number of Zn^{2+} collected from MD simulations in ZBAW15.3.

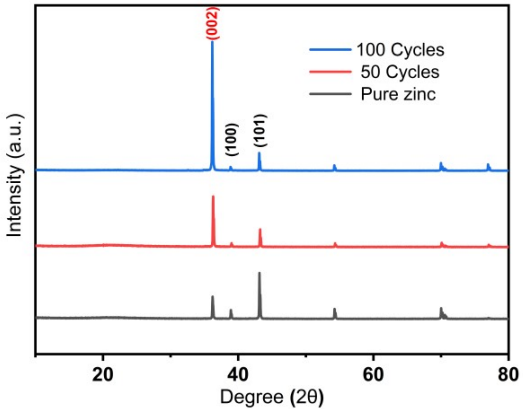

Figure S8. XRD image of Initial, 50 cycles and 100cycles Zn anode in ZBAW15.3.

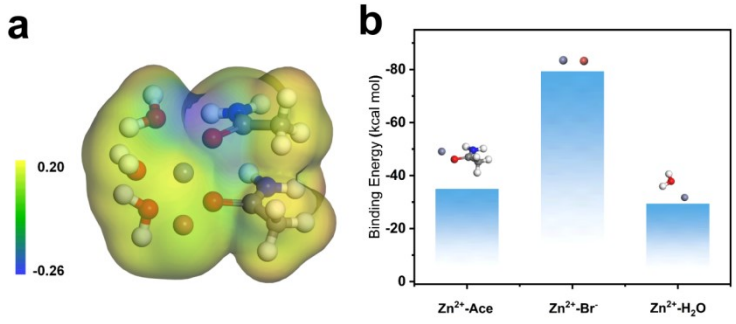

Figure S9. (a) Electrostatic potential map of $[Zn(H_2O)_3(Ace)_2Br]^+$ in ZBAW15.3. (b) Binding energy of Zn-Ace, Zn-H_2O, and Zn-Br in ZBAW15.3.

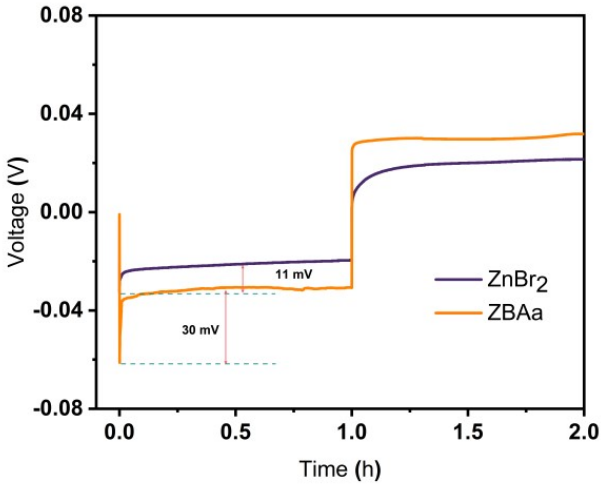

Figure S10. Nucleation overpotentials of electrolytes for aqueous and eutectic systems.

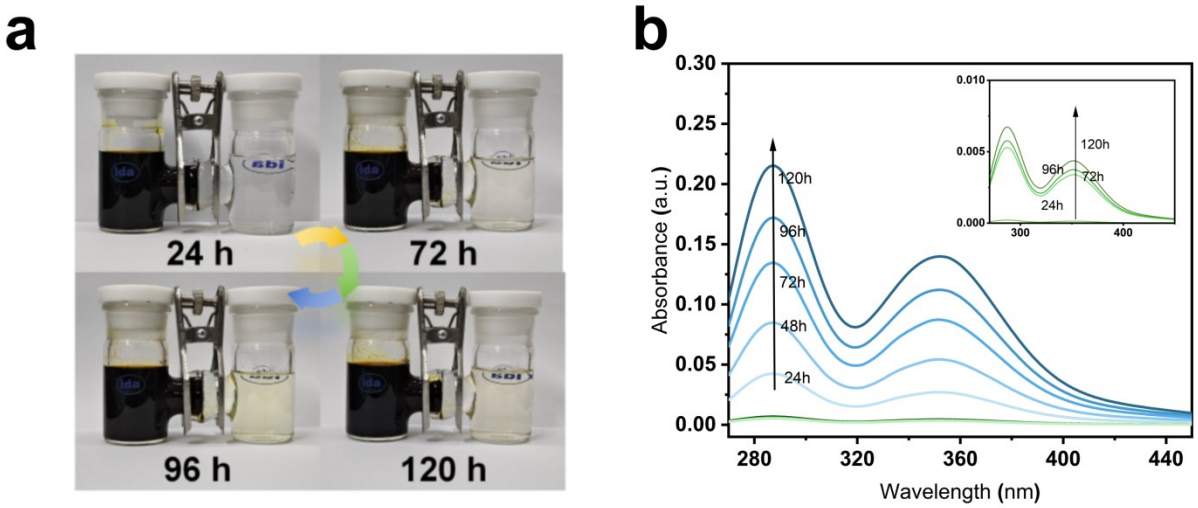

Figure S11. (a). Photographs of the I_3^- permeate solutions through CRIS membranes under ZBA-I electrolytes. (b). UV-vis of the I_3^- permeated side (blue curve - commercial N117 membrane; green curve - CRIS membrane).

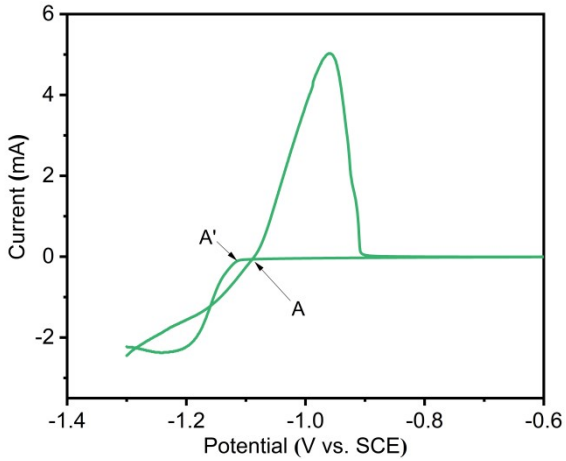

Figure S12. CV curves of Zn in ZBAW15.3.

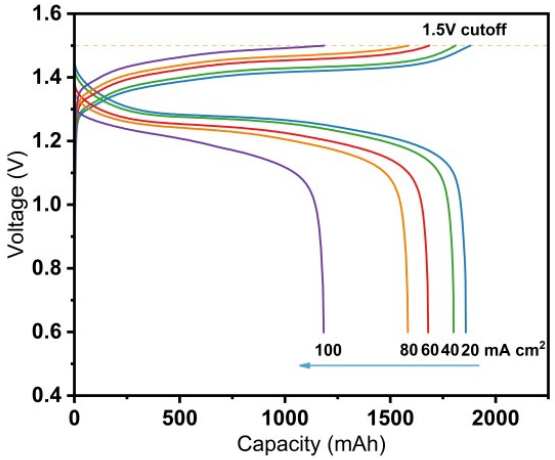

Figure S13. Voltage profiles of ZBAFB in 20-100 mA cm^{-2}.

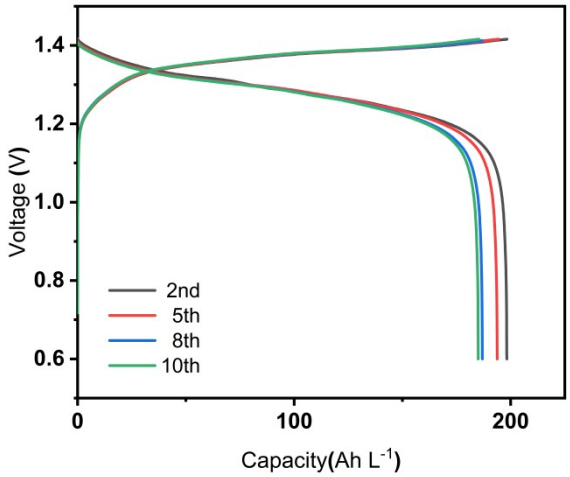

Figure S14. The 2nd, 5th, 8th, and 10th charging/discharging curves of ZBAFB at 10 mA cm^{-1}.

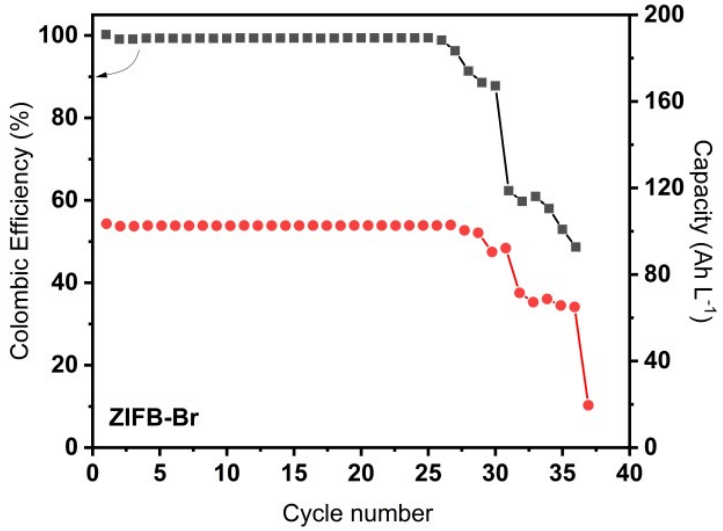

Figure S15. Cyclic performance of ZIFB-Br.

Table S1 The electrolyte costs of ZBAFB.

	Cathode electrolyte			Anode electrolyte		
Chemical materials	I_2	Acetamide	$ZnBr_2$	$ZnBr_2$	Acetamide	Zn
Price [\$ kg^{-1}]	93.79	12.41	20.41	20.41	12.41	96.59 (0.1 mm thickness)
Molar mass (g mol^{-1})	254	59.07	225.2	225.2	59.07	65.39
Concentration (mol L^{-1})	4.0	6.0	2.0	2.0	6.0	2.0
Volume	7mL			14mL		
Volumetric capacity (Ah L^{-1})	192.2			-		
Price (\$ Ah^{-1})	0.57			-		

$$P_{catholyte}(\$ \cdot Ah^{-1}) = (P_S \times C_S + P_A \times C_A) \times \frac{1}{nFC_A}$$

$$P_{catholyte}(\$ \cdot Wh^{-1}) = (P_S \times C_S + P_A \times C_A) \times \frac{1}{nFC_A V}$$

where in the catholyte, the P_S is the cost of the eutectic components (\$ mol^{-1}), C_S is the concentration of eutectic components (mol L^{-1}), P_A is the price of active material (\$ mol^{-1}), C_A is the concentration of the active material (mol L^{-1}), n is the number of charge transfer, F is Faraday's constant, and V is cell voltage.

Table S2 The electrolyte composition of ZBAFB.

	Molar Ratio of Cathode electrolyte				$C(Zn^{2+})$ mol / L	$C(I_2)$ mol / L
	I_2	$ZnBr_2$	Acetamide	H_2O		
1	2.0	1.0	3.0	0	**2.6**	**5.2**
2	2.0	1.0	3.0	6.43	**2.0**	**4.0**

	Molar Ratio of Anode electrolyte			$C(Zn^{2+})$ mol / L
	$ZnBr_2$	Acetamide	H_2O	
1	1.0	3.0	0	**4.45**
2	1.0	3.0	15.3	**2.0**

Table S3 The reported electrolyte comparison of ZIFBs.

Catholyte composition	Current density mA cm^{-2}	CE %	Energy density Wh L^{-1}	Price ($ Ah^{-1})	Reference
KI + KSCN	20	99	165.62	0.82	1
KCl + KI + $ZnBr_2$	80	94	60	1.12	2
NH_4I + NH_4Cl	20	99	137.00	2.01	3
ZnI_2 + NH_4Br	40	99	50.70	3.47	4
ZnI_2 + $ZnBr_2$	10	95	202.00	3.89	5
NaI + PC	20	90	29.51	1.96	6
KI + PVP	20	99	149.50	1.09	7
ZnI_2 + C_2H_6O	10	91	167.00	3.76	8
KI	80	96	205.00	1.03	9
$ZnBr_2$+C_2H_5NO+I_2	20	98	241.18	0.57	This work

Refs:
1. B. Lu, M. Yang, M. Ding, S. Yan, W. Xiang, Y. Cheng, H. Fu, Z. Xu and C. Jia, *SusMat*, 2023, **3**, 522–532.
2. C. Xie, H. Zhang, W. Xu, W. Wang, and X. Li, *Angew. Chem. Int. Ed.*, 2018, **57**, 11081-11469.
3. M. Mousavi, G. Jiang, J. Zhang, A. Kashkooli,H. Dou, C. J. Silva, Z. P. Cano, Y. Niu, A.Yu, and Z. Chen. *Energy Storage Mater.*, 2020, **32**, 465-476.
4. Q. Jian, M. Wu, H. Jiang, Y. Lin, and T. Zhao, *J. Power Sources*, 2021, **484**, 229238-229246.
5. G. Weng, Z. Li, G. Cong, Y Zhou, and Y. Lu, *Energy Environ. Sci.*, 2017, **10**, 735-741.
6. I. Shota; S. Masatoshi, T. Yuichi, O. Akihiro, K. Masaki, and S. Masanori, *Electrochim. Acta.*, 2019, **319**, 164-174.
7. J. Yang, Y. Song,Q. Liu, and A. Tang, *J. Mater. Chem. A*, 2021,**9**, 16093-16098.
8. B. Li, Z. Nie, M. Vijayakumar, G. Li, J. Liu, V. Sprenkle and W. Wang, *Nat. Commun*., 2015, **6**, 6303.
9. R. Amin, A. Abouimrane, U. Nisar, M. Rahman, M. Dixit, and I. Belharouak, *J. Mater. Chem. A,* 2024, 10.1039/D4TA01061B.